

Well-width dependence of optical properties of rare-earth ion-doped $\text{ZnS}_{0.8}\text{Se}_{0.2}$ /undoped ZnS multiple quantum wells

Masanori Tanaka*

*Single Quantum Dot Project, ERATO, Japan Science and Technology Corporation, 5-9-9 Tokodai, Tsukuba 300-2635, Japan*Hisashi Yamada,[†] Takahiro Maruyama,[‡] and Katsuhiro Akimoto
Institute of Applied Physics, University of Tsukuba, Ibaraki 305-8573, Japan

(Received 7 August 2002; published 9 January 2003)

We compare optical properties of Sm^{3+} -doped $\text{ZnS}_{0.8}\text{Se}_{0.2}$ /undoped ZnS multiple-quantum wells (MQWs) with different well widths (2, 5, 10 monolayers) and bulk $\text{ZnS}_{0.8}\text{Se}_{0.2}:\text{Sm}^{3+}$ crystal. The excitonic peak in the photoluminescence excitation spectrum of the Sm^{3+} luminescence shifts to the shorter-wavelength side with reducing well width, which shows that the excitation of Sm^{3+} occurs through the energy transfer from the spatially confined excitons. The activation energy of the thermal quenching of the Sm^{3+} luminescence is found to increase with reducing well width. This result is interpreted as due to the difference in the spatial confinement effect on the binding energy of the free exciton. In addition, the quantum efficiency of the Sm^{3+} luminescence at 4 K is found to increase remarkably with reducing well width. At this temperature, the quantum efficiency of the two monolayers MQW sample is more than 16 times as high as that of the bulk sample. Probable causes of this fact are discussed.

DOI: 10.1103/PhysRevB.67.045305

PACS number(s): 78.55.Et, 81.07.St, 73.20.Hb

I. INTRODUCTION

For the past decade, optical properties of dopant ions as well as of excitons in quantum structures have been studied extensively.^{1–16} As to the luminescence properties of the dopant ions, Bhargava's group³ reported that ZnS nanocrystals doped with manganese ions show very high quantum efficiency of the Mn^{2+} luminescence at room temperature under the interband excitation. This result has attracted much attention in the field of practical phosphors, because, in the case of the interband excitation, a reduction in crystallite size is generally believed to cause a decrease in luminescence quantum efficiency owing to efficient nonradiative recombination of photogenerated electron-hole pairs at the crystalline surfaces. Recently, it has been found that the thermal quenching of the luminescence from Mn^{2+} doped into ZnS and CdS nanocrystals under the interband excitation is much weaker than that in the corresponding bulk crystals, which leads to high luminescence quantum efficiency of the nanocrystal samples at room temperature.^{11,13}

The purpose of this study is to examine how optical properties of dopant ions in quantum wells change from those in the bulk crystal and also with the well width. While there are many reports on the doped zero-dimensional semiconductors (quantum dots or nanocrystals),^{3–11,13–16} studies on the optically active ions doped into two-dimensional systems, such as quantum wells, are very scarce.¹² In this paper, we investigate the luminescence properties of Sm^{3+} -doped $\text{ZnS}_{0.8}\text{Se}_{0.2}$ /undoped ZnS multiple-quantum wells and bulk $\text{ZnS}_{0.8}\text{Se}_{0.2}:\text{Sm}^{3+}$ crystal. The $\text{ZnS}_{0.8}\text{Se}_{0.2}$ /undoped ZnS multiple-quantum wells belong to type I, in which the electrons and holes are both confined within the same well layers.¹⁷ Sm^{3+} is one of the rare-earth ions that are now put to practical uses as the electroluminescence device. Our main attention is paid to the well-width dependence of the

thermal quenching and the quantum efficiency of the Sm^{3+} luminescence.

II. EXPERIMENTS

The Sm^{3+} doped multiple-quantum well (MQW) samples were grown on (001)-oriented GaAs substrates by molecular-beam epitaxy. Detailed procedure of the growth was reported elsewhere.¹² Sm^{3+} was doped into the $\text{ZnS}_{0.8}\text{Se}_{0.2}$ well layers, and not into the ZnS barrier layers. A ZnS buffer layer of 100 nm in thickness was initially grown on the GaAs substrate to reduce dislocations. The MQW structure consists of 100 periods of Sm^{3+} -doped $\text{ZnS}_{0.8}\text{Se}_{0.2}$ wells and 5-nm-thick undoped ZnS barrier with a 20-nm-thick ZnS capping layer. Three kinds of MQW samples were fabricated which have different well widths of 2, 5, and 10 monolayers (ML). The widths of the 2 ML, 5 ML, and 10 ML are 0.54 nm, 1.35 nm, and 2.7 nm, respectively. Bulk $\text{ZnS}_{0.8}\text{Se}_{0.2}$ doped with Sm^{3+} was also prepared as a reference sample. The concentration of Sm^{3+} is the same for the bulk host crystal and the well layers of $\text{ZnS}_{0.8}\text{Se}_{0.2}$ and is of the order of 10^{-2} mole% of Zn^{2+} .

Photoluminescence (PL) spectra were taken with a combination of a 32 cm monochromator (Acton Research, Spectrapro-300i) and a Si-charge-coupled-device detector cooled with liquid nitrogen. For the comparison of the luminescence quantum efficiency between the grown samples, the 325 nm line of a He-Cd laser was used as an excitation source. In the measurement of the temperature dependence of the PL spectra, the excitation was done at 260 nm wavelength. This excitation light was obtained by passing the light from a 500 W xenon lamp through a 25 cm monochromator (JASCO, CT25CP). Photoluminescence excitation (PLE) spectra were also measured in the 280–380 nm wavelength range, by monitoring the luminescence of Sm^{3+} around 650 nm. The samples were mounted on a cold finger of a closed-

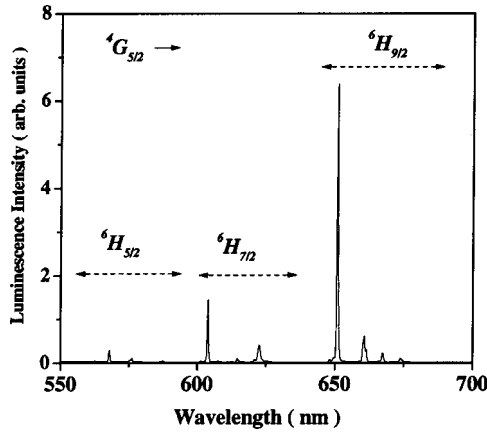


FIG. 1. Photoluminescence spectrum of a $\text{ZnS}_{0.8}\text{Se}_{0.2}:\text{Sm}^{3+}/\text{ZnS}$ multiple-quantum well with two monolayers at 10 K. The excitation was done at 340 nm wavelength. Photoluminescence intensity was corrected for the wavelength dependence of the monochromator and the response of the detector.

cycle He refrigerator (Daikin, UV202CL) or a liquid-He flow-type cryostat (Oxford instrument).

It is important from the crystallographic viewpoint to know where Sm^{3+} is located in each sample and how the charge is compensated. However, the experiments to clarify these questions, such as the measurement of the extended x-ray-absorption fine structure, are beyond the scope of this paper.

III. RESULTS AND DISCUSSION

All the Sm^{3+} doped MQW samples as well as bulk $\text{ZnS}_{0.8}\text{Se}_{0.2}:\text{Sm}^{3+}$ showed many sharp luminescence spectral lines in visible region under the ultraviolet light excitation. In Fig. 1, we show the PL spectrum of the 2ML-MQW sample at 10 K under the excitation at 325 nm wavelength. Since the sharpness of the observed luminescence lines is characteristics of the intra- $4f$ transition of the rare-earth ion in crystals, the luminescence lines are ascribed to the $4f^5-4f^5$ transitions of the Sm^{3+} ion. On the basis of the Dieke's energy-level diagram,¹⁸ the PL spectral lines in the 570–590 nm, 600–625 nm, and 650–675 nm regions can be assigned to the transitions from the $^4G_{5/2}(4f^5)$ state to the $^6H_{5/2}(4f^5)$, $^6H_{7/2}(4f^5)$, and $^6H_{9/2}(4f^5)$ states, respectively. Other samples also exhibit the PL spectra similar to that of the 2ML-MQW sample, and the strength distribution of the transitions is almost the same for all the samples. This fact suggests that all the samples used in this study resemble each other in the crystal-field interaction acting on Sm^{3+} .

Figure 2 shows the PLE spectra of the Sm^{3+} luminescence of a series of MQW samples and bulk $\text{ZnS}_{0.8}\text{Se}_{0.2}:\text{Sm}^{3+}$. A shoulder is observed in the low-energy region of each spectrum. In the PLE spectra of bulk ZnS crystals doped with low concentrations of Mn^{2+} and Sm^{3+} , the peaks were observed at the positions of the free exciton transitions.^{19,20} Similarly, the shoulder in Fig. 2 can be assigned to the excitonic transition of the well layer. As is seen in Fig. 2, the position of the shoulder shifts to shorter wave-

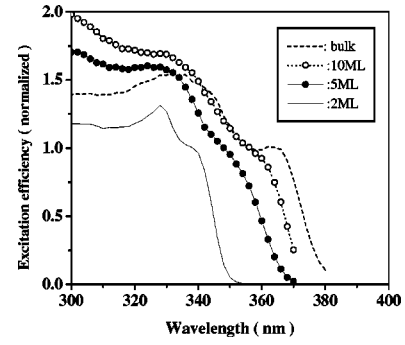


FIG. 2. Photoluminescence excitation spectra of $\text{ZnS}_{0.8}\text{Se}_{0.2}:\text{Sm}^{3+}/\text{ZnS}$ multiple-quantum wells with 2, 5, and 10 monolayers and bulk $\text{ZnS}_{0.8}\text{Se}_{0.2}:\text{Sm}^{3+}$ at 10 K. The most intense $^4G_{5/2}-^6H_{9/2}$ luminescence of Sm^{3+} was monitored in all the samples.

length with reducing well width. This result clearly shows that the luminescence of Sm^{3+} occurs through the free excitons confined in the well layers. Since the exciton Bohr radii of bulk ZnS and ZnSe semiconductors are 2.4 and 3.3 nm, respectively, that of $\text{ZnS}_{0.8}\text{Se}_{0.2}$ is estimated to be about 2.6 nm by the linear-interpolation method on the basis of Vegard's law. Thus, it is quite reasonable that our three MQW samples show the confinement effect of the free exciton. No structures due to the intra- $4f$ shell transitions were observed in the PLE spectra of all the samples, because of the weakness of their transition strengths. This fact shows that the contribution of the direct excitation of Sm^{3+} through the $f-f$ absorption transitions is negligibly small, compared with that of the excitation transfer from the semiconductor host.

Figure 3 shows the temperature dependence of the Sm^{3+} PL intensity at about 650 nm in the 9–305 K range under the excitation at 260 nm wavelength. Since this excitation position is by far higher in energy than the band-gap energies of the bulk $\text{ZnS}_{0.8}\text{Se}_{0.2}$ crystal and the ZnS barrier layers of all the MQW samples, their absorption coefficients at the excitation wavelength are considered to be almost constant in the above temperature

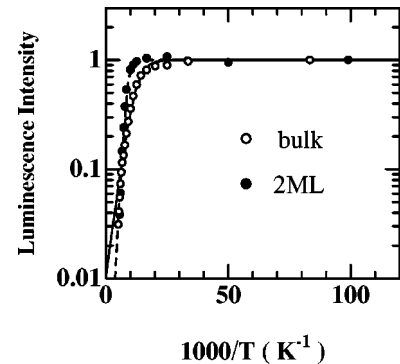


FIG. 3. Temperature dependence of the intensity of the Sm^{3+} luminescence of a 2ML $\text{ZnS}_{0.8}\text{Se}_{0.2}:\text{Sm}^{3+}/\text{ZnS}$ multiple-quantum well and a bulk $\text{ZnS}_{0.8}\text{Se}_{0.2}:\text{Sm}^{3+}$ crystal at about 650 nm. The excitation was done at 260 nm wavelength. The luminescence intensity at 10 K is taken as unity. The broken line and the solid line are the fitted curves for the 2ML multiple-quantum well and bulk $\text{ZnS}_{0.8}\text{Se}_{0.2}:\text{Sm}^{3+}$ crystal, respectively, using Eq. (1).

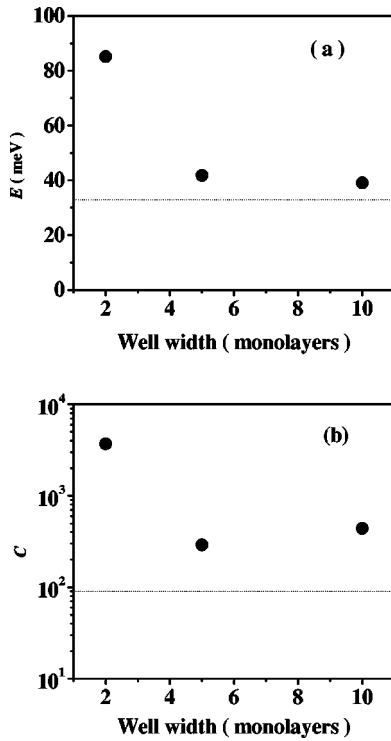


FIG. 4. Well-width dependence of the activation energy E (a) and the preexponential factor C (b) in Eq. (1), which were determined from the thermal quenching behavior of the Sm^{3+} luminescence. For comparison, E and C of a bulk $\text{ZnS}_{0.8}\text{Se}_{0.2}:\text{Sm}^{3+}$ crystal are also shown by the dotted line. Note that the vertical axis in (b) is logarithmic.

range. Thus, the PL intensity in Fig. 3 can be regarded as being proportional to the luminescence quantum efficiency. The experimental data in Fig. 3 are fitted very well with the following expression taking into account one deexcitation channel

$$I(T) = \frac{I(0)}{1 + C \exp(-E/kT)}. \quad (1)$$

Here, E is the thermal activation energy and C is a constant. In Figs. 4(a) and (b), we show the values of E and C obtained from the best fit to the experimental data. E increases monotonically with reducing well width. C varies by two orders of magnitude from one sample to another.

Here let us discuss the origin of the activation energy E . First, we treat the case of bulk $\text{ZnS}_{0.8}\text{Se}_{0.2}:\text{Sm}^{3+}$. There have so far been several studies on the mechanism of the excitation of optically active ions doped into bulk semiconductors. These studies have assumed that an efficient intra- $4f$ shell excitation of the rare-earth ion involves the formation of an exciton bound at the rare-earth ion and subsequent nonradiative decay of the bound exciton by the energy transfer to the ion, and also that an activation energy for the thermal quenching of the PL should correspond to the dissociation (or binding) energy of the excitons bound at the rare-earth ion sites quenches the luminescence of the rare-earth ion. (Here, the dissociation of the bound exciton means a release of a hole, an electron, or a free exciton from the

bound exciton.^{21–23}) However, the activation energy obtained in our bulk sample is fairly large compared with the binding energies of the bound excitons reported so far,^{21–23} but agrees very well with the free exciton dissociation energy 33 meV of bulk $\text{ZnS}_{0.8}\text{Se}_{0.2}$ crystal estimated by the linear-interpolation method. (Here, the dissociation of a free exciton means that a free exciton is thermally liberated to an electron and a hole.) In this estimation, we used the free exciton dissociation energies of 20 and 36 meV for bulk ZnSe and ZnS crystals, respectively.¹ The coincidence between the activation energy and the dissociation energy of the free exciton strongly indicates that the dissociation of the free exciton is responsible for the thermal quenching of the Sm^{3+} luminescence.

One may think that the deexcitation processes at the excited states of Sm^{3+} contribute to the thermal quenching of the luminescence from the $\text{Sm}^{3+} {}^4G_{5/2}$ state in Fig. 3. However, in our samples, this contribution is negligibly small for the following reasons. It is well known that the nonradiative transition between the $4f^n$ states of the rare-earth ion in solids occurs by the multiphonon emission process. The rate of the relaxation process of this type is determined by the highest-energy phonon and the energy separation between the $4f^n$ states concerned with the nonradiative transition.²⁴ The energies of the phonons that couple with the Sm^{3+} ion in our samples are considered to be below 350 cm^{-1} , which corresponds to the energy of the longitudinal-optical phonon of bulk $\text{ZnS}_{0.8}\text{Se}_{0.2}$ crystal.²⁵ The crystal-field levels of Sm^{3+} with the energies higher than the ${}^4G_{5/2}$ state are closely spaced in energy and the energy separations of the neighboring two levels are comparable to or smaller than the longitudinal-optical phonon energy, while the energy separation between the $\text{Sm}^{3+} {}^4G_{5/2}$ state and the next lower ${}^6F_{11/2}$ one is as large as about 7000 cm^{-1} .¹⁸ Because of such an energy-level structure, Sm^{3+} excited by the energy transfer from the excitons relaxes to the ${}^4G_{5/2}$ state of the luminescence initial state nonradiatively with an efficiency of nearly 100%. Furthermore, the radiative relaxation dominates the deexcitation process at the ${}^4G_{5/2}$ state of Sm^{3+} in the measurement temperature range, and the nonradiative relaxation from this state hardly affects the thermal quenching behaviors in Fig. 3. From the above considerations, we can neglect the contribution of the relaxation processes at the excited states of Sm^{3+} to the observed thermal quenching. This discussion also holds good in the MQW samples.

Next, we consider the thermal quenching of the MQW samples. There is a possibility that the thermal escape of the excitons (or carriers) from the well layers to the barriers contributes to the thermal quenching of the Sm^{3+} luminescence in the MQW samples. If this mechanism is responsible for the thermal quenching, the activation energy, which corresponds to the energy separation between the first exciton (or carrier) quantized level of the well layer and the barrier band gap, should decrease with reducing well width. However, this is contrary to the experimental result of Fig. 4(a). Also in the MQW samples, it may be reasonable to attribute the activation energy to the dissociation of the free exciton, as in the case of bulk $\text{ZnS}_{0.8}\text{Se}_{0.2}:\text{Sm}^{3+}$. If this speculation is correct, we expect that the activation energy increases with re-

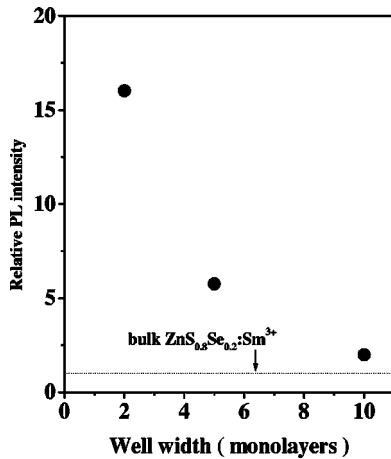


FIG. 5. Well-width dependence of the luminescence intensity of Sm^{3+} at about 650 nm relative to bulk $\text{ZnS}_{0.8}\text{Se}_{0.2}:\text{Sm}^{3+}$ at 4 K. The luminescence intensity of bulk $\text{ZnS}_{0.8}\text{Se}_{0.2}:\text{Sm}^{3+}$ is taken as unity. The excitation was done at 325 nm wavelength.

ducing well width, because of the spatial confinement effect on the free exciton dissociation (or binding) energy. Our experimental result coincides with this expectation. The theoretical value of the binding energy in the limit of a two-dimensional exciton is known to be increased by a factor of 4 relative to the three-dimensional case.¹⁷ However, if we take into account the penetration of the exciton wave function of the well layer into the barrier layer and the thickness of the well layer, it is predicted that the ratio of the dissociation energy of the free exciton is a little smaller than the factor 4. On the other hand, from Fig. 4, the ratio of the activation energy of the 2ML sample to that of the bulk crystal is found to be about 2.6, which is slightly smaller than 4. This fact supports further the attribution of the activation energy to the dissociation energy of the free exciton. On the basis of the above discussions, the difference in the activation energy E of the thermal quenching behavior among our samples is ascribed to the spatial confinement effect on the dissociation (or binding) energy of the free exciton.

In Fig. 5, we show the well-width dependence of the intensity of the Sm^{3+} luminescence at 4 K under the excitation at 325 nm. Here, the luminescence intensity is normalized by the well width. It should be noted that the PL intensity increases remarkably with reducing well width. The Sm^{3+} luminescence of the 2ML-MQW sample is 16 times stronger than that of bulk $\text{ZnS}_{0.8}\text{Se}_{0.2}:\text{Sm}^{3+}$. Since the band-gap energy of the well layer becomes high with the reduction of the well width due to the quantum confinement, the optical density at the above excitation position should be lower for the sample with narrower well width. Accordingly, as the well-width decreases, the luminescence quantum efficiency is expected to increase at higher rate than the PL intensity shown in Fig. 5. This result is similar to the dependence of the luminescence quantum efficiency of $\text{ZnS}:\text{Mn}^{2+}$ and $\text{ZnSe}:\text{Mn}^{2+}$ nanocrystals on the crystallite size.^{3,7} Since, at 4 K, the thermal dissociation of the free exciton hardly occurs, the luminescence quantum efficiency at this temperature is proportional to the rate of the energy transfer from the exci-

ton to the ion. Thus, Fig. 5 implies that the rate of the energy transfer from the exciton to Sm^{3+} becomes high with the reduction of the well width.

A probable cause of such an enhancement of the energy-transfer rate is an increase in the squared overlap integral of the wave functions of an electron and a hole in the well layers due to the spatial confinement, as explained below. The squared transition matrix element of the free exciton is given by $|\mu|^2|U(0)|^2$. Here, μ is the transition dipole moment, and $|U(0)|^2$ represents the probability of finding an electron and a hole at the same site (or the squared overlap integral of the electron and hole wave functions). As the well width is reduced, the exciton size is decreased and accordingly $|U(0)|^2$ is increased.^{1,14} According to the energy-transfer theory of Dexter,²⁶ the rate of the energy transfer from the exciton to Sm^{3+} may be proportional to $|\mu|^2|U(0)|^2$. Consequently the energy-transfer rate is enhanced with reducing well width. The theoretical value of the exciton size in the limit of a two-dimensional crystal is known to be decreased by a factor of 2 compared with the three-dimensional case.¹⁷ Correspondingly, the value of $|U(0)|^2$ in the two-dimensional crystal is eight times as large as that of the bulk crystal. This quantitative estimation suggests that the data in Fig. 5 can not be explained completely only in terms of the spatial confinement effect of the electron and hole. Thus, besides this effect, there should exist additional causes for the increase in the luminescence efficiency with reducing well width. To our regret, these causes have not been clarified yet.

Finally, we pay our attention to the preexponential factor C in Eq. (1). C is proportional to the ratio of the nonradiative deexcitation rate K_{nr} at high temperatures to the energy-transfer rate from the free exciton to Sm^{3+} . From the data of Figs. 4(b) and 5, K_{nr} is found to increase monotonically and largely with the reduction of the well width. K_{nr} of the 2ML sample is increased by three orders of magnitude compared with bulk $\text{ZnS}_{0.8}\text{Se}_{0.2}:\text{Sm}^{3+}$ crystal. At high temperatures, the free excitons are dissociated thermally, which increases the rate of nonradiative carrier recombination on defect centers.²⁷ K_{nr} is, thus, related to the density of the defect centers. The density of the defect centers is usually high at the $\text{ZnS}_{0.8}\text{Se}_{0.2}/\text{ZnS}$ interface. Accordingly, the increase in K_{nr} with reducing well width can be understood as being caused by the increase in the defect center density due to the increase in $\text{ZnS}_{0.8}\text{Se}_{0.2}/\text{ZnS}$ interface-to-volume ratio.

IV. SUMMARY

In summary, we have examined the optical properties of Sm^{3+} -doped $\text{ZnS}_{0.8}\text{Se}_{0.2}/\text{ZnS}$ MQWs with 2, 5, and 10 monolayers and bulk $\text{ZnS}_{0.8}\text{Se}_{0.2}:\text{Sm}^{3+}$. Under the band-to-band excitation of the ZnS barrier layer of the MQW samples and the bulk $\text{ZnS}_{0.8}\text{Se}_{0.2}$ host crystal, the luminescence quantum efficiency of Sm^{3+} at 4 K has been found to increase remarkably with reducing well width. The quantum efficiency of the two monolayers MQW sample at 4 K is more than 16 times as high as that of the bulk sample. One of probable causes for this result has been shown to be the

significant increase in the rate of the energy transfer from the free exciton to the Sm^{3+} ion with the reduction of the well width. It has been found that the thermal quenching behavior of the Sm^{3+} luminescence depends largely on the well width. The activation energy obtained from the thermal

quenching characteristic has been assigned to the dissociation energy of the free exciton in all the samples. The difference of the activation energy among the samples has been understood as due to the spatial confinement effect on the dissociation energy of the free exciton.

*Corresponding author, Present address: Research Institute for Green Technology, National Institute of Advanced Industrial Science and Technology, 16-1, Onogawa, Tsukuba 305-8569, Japan.

[†]Present address: Sumitomo Chemical Co., Ltd, Tsukuba Research Laboratory, 6 Kitahara, Tsukuba 300-3294 Japan.

[‡]Present address: Dept. of Photonics, Ritsumeikan University 1-1 Noji-Higashi, Kusatsu, Shiga 525-8577, Japan.

¹A.D. Yoffe, *Adv. Phys.* **42**, 173 (1993).

²For a review, see J. Lumin. **70** (1996), Special Issue on Spectroscopy of Isolated and Assembled Semiconductor Nanocrystals, edited by L.E. Brus, A.L. Efros, and T. Itoh.

³R.N. Bhargava, D. Gallagher, X. Hong, and A. Nurmikko, *Phys. Rev. Lett.* **72**, 416 (1994).

⁴I. Yu, T. Isobe, and M. Senna, *J. Phys. Chem. Solids* **57**, 373 (1996).

⁵K. Sooklal, B.S. Cullum, S.M. Angel, and C.J. Murphy, *J. Phys. Chem.* **100**, 4551 (1996).

⁶U. Hömmerich, F. Namavar, A. Cremers, and K. Bray, *Appl. Phys. Lett.* **68**, 1951 (1996).

⁷Y. Wu, K. Arai, N. Kuroda, T. Yao, A. Yamamoto, M. Shen, and T. Goto, *Jpn. J. Appl. Phys., Part 2* **36**, L1648 (1997).

⁸A.A. Bol and A. Meijerink, *Phys. Rev. B* **58**, R15 997 (1998).

⁹N. Murase, R. Jagannathan, Y. Kanematsu, M. Watanabe, A. Kurita, K. Hirata, T. Yazawa, and T. Kushida, *J. Phys. Chem. B* **103**, 754 (1999).

¹⁰M. Tanaka, J. Qi, and Y. Masumoto, *J. Lumin.* **87-89**, 472 (2000).

¹¹M. Tanaka, J. Qi, and Y. Masumoto, *J. Cryst. Growth* **214/215**, 410 (2000).

¹²H. Yamada, M. Tanaka, T. Maruyama, Y. Masumoto, T. Yao, and

K. Akimoto, *J. Cryst. Growth* **214/215**, 935 (2000).

¹³M. Tanaka and Y. Masumoto, *Chem. Phys. Lett.* **324**, 249 (2000).

¹⁴W. Chen, R. Sammynaiken, and Y. Huang, *J. Appl. Phys.* **88**, 5188 (2000).

¹⁵W. Chen, R. Sammynaiken, Y. Huang, J. Malm, R. Wallenberg, J. Bovin, V. Zwiller, and N.A. Kotov, *J. Appl. Phys.* **89**, 1120 (2001).

¹⁶M. Tanaka and Y. Masumoto, *Solid State Commun.* **120**, 7 (2001).

¹⁷P. Y. Yu and M. Cardona, *Fundamentals of Semiconductors* (Springer-Verlag, Berlin, 1996), p. 457.

¹⁸G.H. Dieke and H.M. Crosswhite, *Appl. Opt.* **2**, 675 (1963).

¹⁹T. Hoshina and H. Kawai, *Jpn. J. Appl. Phys.* **19**, 267 (1980).

²⁰M. Tanaka, H. Yamada, T. Maruyama, and K. Akimoto (unpublished).

²¹H. Przybylińska, K. Świątek, A. Stąpor, A. Suchocki, and M. Godlewski, *Phys. Rev. B* **40**, 1748 (1989).

²²K. Świątek, M. Godlewski, and D. Hommel, *Phys. Rev. B* **42**, 3628 (1990).

²³K. Świątek, M. Godlewski, and D. Hommel, *Phys. Rev. B* **43**, 9955 (1991).

²⁴See, for example, B. Henderson and G. F. Imbusch, *Optical Spectroscopy of Inorganic Solids* (Clarendon, Oxford, 1989), p. 183.

²⁵O. Brafman, I.F. Chang, G. Lengyel, S.S. Mitra, and E. Carnall, *Phys. Rev. Lett.* **19**, 1120 (1967).

²⁶D.L. Dexter, *J. Chem. Phys.* **21**, 836 (1953).

²⁷H. Przybylinska, W. Jantsch, Y. Suprun-Belevitch, M. Stepikhova, L. Palmetshofer, G. Hendorfer, A. Kozanecki, R.J. Wilson, and B.J. Sealy, *Phys. Rev. B* **54**, 2532 (1996).